Field Crops Research 244 (2019) 107619

Contents lists available at ScienceDirect

Field Crops Research

journal homepage: www.elsevier.com/locate/fcr

Linkage disequilibrium mapping of high-throughput image-derived descriptors of plant architecture traits under field conditions

Matthew W. Breitzman[a], Yin Bao[b], Lie Tang[b], Patrick S. Schnable[a], Maria G. Salas-Fernandez[a,*]

[a] Department of Agronomy, Iowa State University, Ames, Iowa, United States
[b] Department of Agricultural and Biosystems Engineering, Iowa State University, Ames, Iowa, United States

ARTICLE INFO

Keywords:
Sorghum
High-throughput phenotyping
Plant architecture
Stereo vision
3D reconstruction
Plant height
Leaf angle

ABSTRACT

Plant architectural traits are important factors in determining grain and biomass productivity of sorghum (*Sorghum bicolor* (L) Moench). However, collecting data on these architectural traits is labor-intensive and time-consuming, especially when using numerous lines in quantitative genetic studies or breeding programs. Therefore, we used the high-throughput field-based robotic platform PhenoBot 1.0 to collect whole canopy stereo images from a large association mapping panel under field conditions. These images were used to create a plot-based 3D reconstruction of the canopy from which phenotypic features were automatically extracted. These features included: plot-based plant height (PPH), plot-based plant width (PPW), plant surface area (PSA), and convex-hull volume (CHV). A small sub-set of sorghum lines were used to obtain ground-truth measurements to validate the image-derived descriptors, and determine their biological significance. PPH was highly correlated with manually measured plant height; PPW correlated with SinAL, defined as leaf length multiplied by the sine of its angle; PSA was associated with manually measured total plant surface area; and CHV was a function of both flag-leaf height and SinAL. Association mapping of PPH identified chromosomal regions containing known plant height genes, confirming the accuracy of the automatic feature extraction process. For the other phenotypic features, significant markers were identified within genomic regions that have been previously reported to control plant architectural characteristics in sorghum such as tiller number, shoot compactness, leaf length, surface area, and angle. The image processing method used in this study contributes new knowledge to the development of high-throughput phenotyping techniques and represents a novel tool for plant breeders.

1. Introduction

Plant architectural features are important components of crop yield. For example, the architectural traits of sorghum (*Sorghum bicolor* (L) Moench), could be manipulated to optimize grain, forage, or biomass yields for biofuel production. Plant height is one of the best characterized phenotypes, and a relatively simple target for the genetic improvement. Biomass sorghums are three to four times taller than grain types, and have proportionally higher biomass yields (Mullet et al., 2014; Olson et al., 2012). Biomass yield of tall plants can be further increased by having greater stem dry mass, which provides a larger sink capacity for carbohydrate accumulation (Brenton et al., 2016; Mullet, 2017; Murray et al., 2008). Leaf angle and leaf area affect photosynthetic efficiency (Mantilla-Perez and Salas Fernandez, 2017; Mullet et al., 2014; Olson et al., 2012). Indeed, improved solar radiation interception as a consequence of altered leaf angles has been reported to result in a 3% gain in sorghum biomass yield (Truong et al., 2015). Similarly, abundant evidence demonstrates that erect leaves generate improvements in grain yields across cereals (Austin et al., 1976; Morinaka et al., 2006; Parry et al., 2011; Sinclair and Sheehy, 1999). For example, in maize (*Zea mays* L.), upright leaves have more than doubled the relative efficiency of CO_2 fixation, improved dry matter accumulation by ~15%, and allowed for higher planting densities, thereby increasing grain yield per unit of land (Lee and Tollenaar, 2007; Pendleton et al., 1968).

The process of manually phenotyping architectural components is time-consuming and labor-intensive (Furbank and Tester, 2011). Bao et al. (2018) found that, depending on growth stage, 32 to 64 person-hours were necessary to collect manual measurements of eleven traits in 18 sorghum plots. Alternatively, these plots could be imaged within three minutes using a high-throughput phenotyping (HTP) platform (Bao et al., 2018). The extensive time required to conduct manual phenotyping has a negative impact on the quality and reproducibility of the data. For instance, when growing cotton (*Gossypium hirsutum* L.)

* Corresponding author.
E-mail address: mgsalas@iastate.edu (M.G. Salas-Fernandez).

https://doi.org/10.1016/j.fcr.2019.107619
Received 20 March 2019; Received in revised form 29 August 2019; Accepted 1 September 2019
Available online 03 October 2019

under water-limited and well-watered conditions, Andrade-Sanchez et al. (2014) found that the normalized difference vegetation index (NDVI) of these treatments decreased by 21% and 7%, respectively, over the course of five hours, suggesting that leaves wilted throughout the day and exposed more soil surface (Andrade-Sanchez et al., 2014). Considering that, it can take several days to complete the manual collection of data from hundreds of genotypes in the field, and that certain phenotypes are affected by variable environmental conditions (wind, sun angle, temperature, humidity) and the circadian clock, HTP techniques have emerged as the best approach to obtain accurate data quickly.

Phenotyping in a greenhouse or growth chamber allows for control over environmental (e.g. day length, temperature, water, fertilizer) and imaging conditions (e.g. single plant, no wind, multiple imaging angles), positively affecting the accuracy of the data. To date, HTP studies have been performed under controlled conditions in maize (Ge et al., 2016; Zhang et al., 2017), barley (*Hordeum vulgare* L.) (Chen et al., 2014; Paulus et al., 2014), wheat (*Triticum aestivum* L.), grapevine (*Vitis vinifera* ssp. *vinifera*) (Wahabzada et al., 2015), tomato (*Solanum lycopersicum*), tobacco (*Nicotiana benthamiana*), and sorghum (Conn et al., 2017; McCormick et al., 2016; Neilson et al., 2015). However, Poorter et al. (2016) analyzed 17 experiments conducted on several species, and discovered only a moderate correlation (r = 0.51) between phenotypes collected in controlled and field conditions for traits such as leaf area, nitrogen concentration, and yield. Therefore, it is critical to deploy these novel HTP systems in field experiments, and invest in new designs to expand the phenotyping portfolio of sensors and platforms.

Several HTP systems are available to collect data on a wide range of characteristics. Multi-sensor platforms have been used to measure or predict traits such as biomass yield, plant moisture content, canopy temperature, canopy reflectance, NDVI, chlorophyll fluorescence, and architectural features in triticale (*XTriticosecale Wittmack* L.) (Busemeyer et al., 2013), cotton (Andrade-Sanchez et al., 2014), soybean (*Glycine max* L. Merr), and wheat (Bai et al., 2016; Comar et al., 2012; Crain et al., 2016; Virlet et al., 2017). In sorghum, a multispectral camera has been used to determine NDVI, enhanced vegetation index (EVI), and normalized difference red edge index (NDRE), which were good estimators of conventional traits such as canopy cover, leaf area index, and leaf chlorophyll content (Potgieter et al., 2017). The use of either red, green, blue (RGB) stereo cameras or high-precision laser scanners have been preferred for several plant architectural traits (Großkinsky et al., 2015; Rahaman et al., 2015). Guo et al. (2018) utilized RGB images collected with unmanned aerial vehicles (UAVs) to phenotype panicle number in sorghum, an important determinant of grain yield. Wang et al. (2018) equipped a high-clearance sprayer with four types of cameras/sensors to evaluate their ability to quickly phenotype the heights of young sorghum plants at a plot level. However, a high-clearance vehicle will not be functional at later developmental stages or for tall biomass sorghum that can reach over four meters in height. To bypass this problem, several groups have used UAVs with RGB cameras to phenotype plant height under field conditions (Hu et al., 2018; Pugh et al., 2018; Watanabe et al., 2017). However, depending on the type of material, and growth stage, accuracies have varied widely (r = 0.4 – 0.95) (Pugh et al., 2018).

Functional limitations of systems developed for short-stature crops and accuracy problems observed with UAVs have triggered the development of specialized ground-based platforms for biomass crops. Several robotic phenotyping devices have been created for imaging within the sorghum canopy. Mueller-Sim et al. (2017) developed the Robotanist, an autonomous mobile sensor platform capable of navigating between crop rows. This system is equipped with light detection and ranging (LiDAR), RGB stereo cameras, and a robotic manipulator with the ability to perform contact-based stalk strength measurements. Sodhi et al. (2017) developed a similar system in which the robot navigates between plots and collects 2D images from multiple heights and viewpoints using stereo cameras. In their work, a 3D plant reconstruction was created and structural traits, such as stem diameter, leaf length, area, and angle were subsequently extracted. However, the rows had to be pruned prior to data collection to avoid occlusion of the cameras, so only one plant appeared in each image. Our research team developed PhenoBot 1.0, a self-propelled platform equipped with RGB stereo cameras capable of collecting 2D images (Bao et al., 2018; Salas Fernandez et al., 2017). In PhenoBot 1.0, after 3D reconstruction of the canopy, image-derived descriptors of architectural components were algorithmically extracted. To avoid occlusion of cameras, an alternative planting design with wider row spacing was adopted. The measurement accuracy of this technology in terms of plot-based plant height, plot-based plant width, convex hull volume, plant surface area, and stem diameter has been validated (Bao et al., 2018; Salas Fernandez et al., 2017).

While the list of studies introducing HTP technologies is growing, their applications to identify genomic regions controlling phenotypes of interest are limited. Quantitative trait loci (QTL) mapping has been performed on field-based HTP in rice (*Oryza sativa*) for yield component traits (Tanger et al., 2017), and in cotton for canopy temperature, NDVI, and plant height (Pauli et al., 2016). Yang et al. (2014) used a genome-wide association study (GWAS) to explore the genetic variation in rice for 15 agronomic and growth-related traits collected using a specially designed HTP facility. In sorghum, QTL regulating shoot architecture at multiple developmental stages were discovered under controlled conditions using a depth camera (McCormick et al., 2016). PhenoBot 1.0 is the only field-based system that has been deployed in sorghum for the discovery of genomic regions controlling plant height and stem diameter using a GWAS (Salas Fernandez et al., 2017).

In this study, we have leveraged the PhenoBot 1.0 platform with the following objectives: i) Test algorithms for the extraction of novel plant architectural parameters; ii) Validate image-derived descriptors via comparisons with manually collected ground-truth data; and iii) Discover genomic regions controlling the natural variation of these novel architecture parameters, based on a GWAS.

2. Materials and methods

2.1. Plant materials and field design

In 2014, the previously described and characterized (Casa et al., 2008; Mantilla Perez et al., 2014; Morris et al., 2013; Salas Fernandez et al., 2017; Zhao et al., 2016) sorghum association panel (SAP), which consists of 325 accessions, was evaluated in two locations in a randomized complete block design with two replications per accession. The testing sites were the Agricultural Engineering and Agronomy Research Farm (AEARF) (Boone, IA), and Curtiss Farm (Ames, IA), planted on May 30 and June 12, respectively. Each accession was grown in a 3 m long two-row plot with a 1.5 m spacing between rows, and a 2.2 m spacing between plots. Considering that the SAP includes both short grain-type and tall forage-type accessions, blocks were divided by sorghum type to reduce uneven competition due to height differences.

In 2016, three grain-type sorghums (PI's: 533902, 534021, and 655990) and three forage-type sorghums (PI's: 655974, 656014, and 656095) were planted on June 7 at AEARF with the same field design used in 2014. This sub-set of genotypes was selected as a representative sample of the SAP diversity for ground-truth validation.

2.2. Data acquisition

In 2014, plot imaging was conducted using PhenoBot 1.0, a field-based robotic platform previously reported by Salas Fernandez et al. (2017) and Bao et al. (2018). PhenoBot 1.0 navigated between the two-row plots collecting images simultaneously from plots on each side. The images utilized for the GWAS were collected 87 and 83 days after planting (DAP) for the AEARF and Curtiss Farm, respectively, while the biomass was obtained 159 and 138 DAP. A John Deere 5730 self-

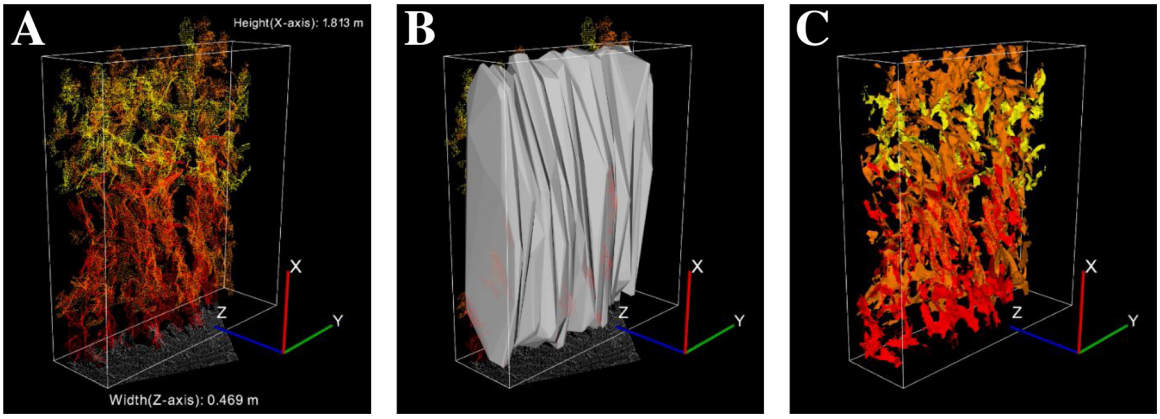

Fig. 1. Image-derived descriptors. A. Plot-Based Plant Height and Width: Axis-aligned bounding box fitted to 3D point cloud. B. Convex-Hull Volume: Convex-hulls fitted to slices of 3D point cloud. C. Plant Surface Area: Triangle mesh surface representation. Different colors represent the point clouds of each of the three stereo cameras sets on Phenobot 1.0 (Bao et al., 2018).

propelled forage harvester with a Wintersteiger weighing system was used to harvest and record wet biomass (WB) weights for each plot. After weighing, the biomass was ejected from the weighing bucket onto the ground. Subsequently, a small biomass sample was collected to obtain water content, by drying to constant weight, to provide an estimate of dry biomass (DB) yield.

In 2016, PhenoBot 1.0 was used to image plots during grain filling. Simultaneously, manual measurements were collected 98 DAP on three representative plants per accession for ground-truth validation.

2.3. Image-derived descriptors

A full description of image processing and data extraction has been reported by Bao et al. (2018). Briefly, the 3DMST algorithm (Li et al., 2017) was used to reconstruct 3D point clouds of the sorghum canopy. The point cloud was fitted with an axis-aligned bounding box (AABB) which had an x-axis parallel to the canopy height, a y-axis along the planting direction of the crop row, and a z-axis spanning the distance from the plant stem into the inter-row space (Fig. 1). However, utilizing a single maximum value for the x and z-axes could result on data of an outlier plant being used as a plot descriptor. Therefore, the AABB was partitioned into 20 equal slices along the y-axis, and each slice was given a statistical weight to reduce the contribution of plot sections with abnormal densities or empty spaces. The statistical weight was determined by the ratio between the slice number of points and the plot total number of points. Finally, the maximum x and z-axes values and the minimum z-axis value of each slice were determined, and once each slice weight was accounted for, a weighted median value was obtained for the entire plot. The minimum x-axis value of the AABB was determined by fitting a plane to the ground points and then computing the x coordinate of the centroid of the ground inliers. The ground surface was robustly identified by plane fitting with random sample consensus (RANSAC). Because the ground plane was approximately perpendicular to the X-axis, the maximum deviation between the randomly sampled plane normal direction and the X-axis was limited to 20°. Any point within 3 cm to the plane was considered as inliers. After the RANSAC plane fitting, the inliers of the ground surface were removed from the point cloud. Xground was computed as the average of the X coordinates of the ground inliers to serve as the reference for measuring plant height. From the AABB, *plot-based plant height* (PPH) and *plot-based plant width* (PPW) were extracted as the height from the bottom to the top of the AABB along the x-axis, and the width on the z-axis, respectively (Fig. 1A).

To estimate canopy volume, the smallest convex path surrounding all 3D points (convex hull), was fitted to each slice (Fig. 1B). A convex hull was considered valid if the ratio of its volume to the slice volume was ≥ 0.3. Additionally, an image had to contain at least eight valid convex hulls out of 20 possible to be included in the analysis. The sum of volumes from all valid convex hulls resulted in the CHV descriptor. Finally, *plant surface area* (PSA) was determined by converting the 3D point cloud into a triangle mesh surface representation (Fig. 1C). The area of every triangle in the mesh was summed to create PSA, which includes all leaves, stems, and panicles of the plot.

2.4. Manual ground-truth measurements

The following plant architecture parameters were manually measured for the ground-truth validation of image-derived descriptors: 1) *plant height*, the distance from the ground to the top of the panicle (Fig. 2A); 2) *flag leaf height*, the distance up to the collar of the flag leaf;

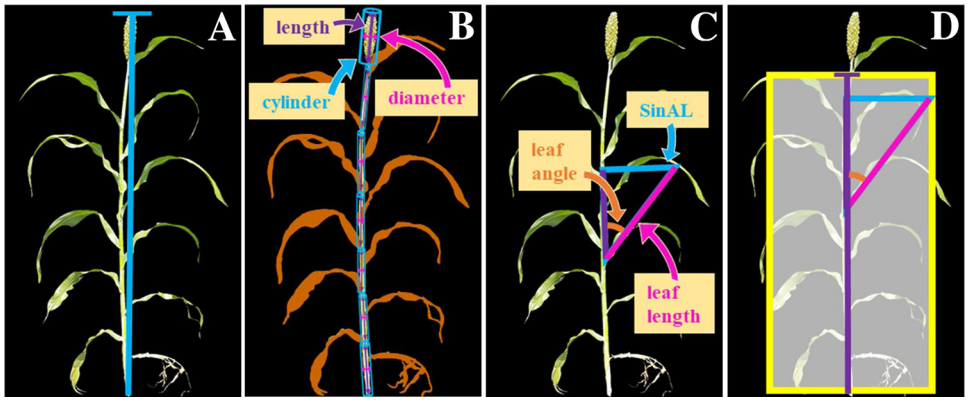

Fig. 2. Manually measured traits. A. Plant height: distance from ground to the top of panicle. B. Plant surface area: sum of surface areas of leaves (orange), stem, and panicle. C. SinAL (blue): sine of the leaf angle multiplied by leaf length (pink). D. Plant occupied area (yellow box): Flag leaf height (purple) multiplied by SinAL (blue). (For interpretation of the references to colour in this figure legend, the reader is referred to the web version of this article).

3) *panicle surface area*, the area of a cylinder determined by the panicle width at its widest point, and the length from the lowest branch node to the panicle tip (Fig. 2B); 4) *stem surface area*, approximated in two-internode sections as the area of an elliptical cylinder, with a perimeter determined by the long and short diameters, before removal of the leaf sheath; 5) *leaf area*, measured using a LI-3100 leaf area meter (LI−COR, Lincoln, NE, USA) for each individual leaf; 6) *leaf length*, from the collar to the tip along the midrib of each detached leaf; and 7) *leaf angle*, between the adaxial midrib and stem for each individual leaf (Fig. 2C). These variables were used to estimate derived traits including 1) *average stalk-leaf tip distance*: the mean stalk-leaf tip distance parallel to the ground on plants standing naturally in the plot; 2) *total leaf surface area*: sum of leaf area for all leaves; 3) *plant surface area*: sum of panicle area, stem area, and total leaf surface area; 4) *average leaf angle*: mean angle across all leaves; 5) *average leaf length*: mean length across all leaves; 6) *SinAL*: the *Sine* of the average leaf *Angle* multiplied by the average leaf *Length*, which represents the triangle side opposite to leaf angle (Fig. 2C); and 7) *plant occupied area*: flag leaf height multiplied by SinAL (Fig. 2D).

2.5. Statistical analysis

Phenotypic data collected in 2014 were analyzed using PROC MIXED in SAS version 9.4 (SAS Institute, 2008) according to the following model: $Y_{ijk} = \mu + L_i + R_{(i)j} + G_k + LG_{ik} + \varepsilon_{ijk}$, where Y_{ijk} is the response variable, μ is the overall mean, L_i is the location effect, $R_{(i)}j$ is the replication nested within the location effect, G_k is the genotype effect, LG_{ik} is the genotype by location interaction, and ε_{ijk} is the residual. All effects were treated as random factors.

Heritability was calculated for each trait using the formula: $H^2 = \sigma^2_G/[\sigma^2_G + (\sigma^2_{GE}/n) + (\sigma^2_e/(nr))]$, where σ^2_G is the genotypic variance, σ^2_{GE} is the genotype x environment interaction variance, σ^2_e is the error variance, *n* is the number of environments, and *r* is the number of replications. Best linear unbiased predictions (BLUPs) were calculated using the R package lme4 with the following linear model: Y = (1|Genotype) + (1|Loc) + (1|Loc/Rep) + (1|Genotype:Loc) + (PPH), where Y is the trait data, 1| indicates random effects, and colon (:) denotes interaction. Genotype corresponds to the 325 sorghum accessions, Loc refers to the two locations, and Loc/Rep designates replications nested within location. PPH indicates the parameter was used as a covariate in the mixed linear model (MLM) for GWAS of CHV and PSA. Correlation coefficients were calculated using BLUPs (without covariates) and Pearson's statistics with the cor procedure in R (R Core Development Team, 2013).

Correlations between manual measurements and image-derived descriptors were calculated for the 2016 dataset using Pearson correlation coefficient. This analysis was used to verify the biological significance of the plant architecture parameters produced by computer algorithms.

2.6. Genome-wide association study

The SAP was previously genotyped using genotyping-by-sequencing (GBS) as reported by Morris et al. (2013). Markers covering genes for brassinosteroids, gibberellins, photosynthesis, photoprotection, and *Dw3* on chromosome 7 have been added to the dataset, as previously described by Mantilla Perez et al. (2014), Zhao et al. (2016) and Ortiz et al. (2017). All marker positions presented are relative to the version 1.4 assembly of the sorghum reference genome (Department of Energy-Joint Genome Institute [http://phytozome.jgi.doe.gov]). A total of 133,910 single nucleotide polymorphisms (SNPs) were evaluated after accounting for a minor allele frequency (MAF) > 5% and missing data < 40%. MLM, as implemented in TASSEL software version 5.2.39 (Bradbury et al., 2007), was utilized to test associations between genotypic variants and phenotypic data (BLUPs). To minimize false-positive associations, MLM uses population structure (Q), as a fixed effect, and kinship (K), as a random effect (Zhang et al., 2010), which were estimated as described by Zhao et al. (2016). Both the Bonferroni method (Duggal et al., 2008) and false discovery rate (FDR) (Storey and Tibshirani, 2003) were applied to adjust for false-positive associations due to multiple testing. The Bonferroni threshold corresponds to a p-value = 3.734e-7 for α = 0.05 and 133,910 tests. The q-value for the FDR was determined individually for each trait using the qvalue package in R (R Core Development Team, 2013). The average extent of linkage disequilibrium (LD) decay to background levels ($r^2 < 0.1$) per chromosome for the SAP (Morris et al., 2013) was used to identify the number of genomic regions encompassing significant markers. These regions were then compared to previously identified QTL for sorghum architectural features and biomass yield using the Sorghum QTL Atlas (Mace et al., 2019).

3. Results

3.1. Phenotypic analysis

Descriptive statistics confirmed the large variability of all image-derived descriptors in the SAP and the sub-set of lines used for ground-truth validation (Table 1). The broad-sense heritability, estimated as repeatability, was calculated for the complete set of 325 accessions, and all image-derived parameters had high values (Table 1). Analysis of variance on this complete data set demonstrated that genotype and genotype by location interaction effects were significant for all image-derived descriptors as well as biomass yield (Supplementary Table 1). For the validation subset, only the genotype effect was significant for all image-derived parameters, while the replication was only significant for PSA, demonstrating that these six genotypes were adequately selected to represent the phenotypic variability within the SAP (Supplementary Table 2).

Correlations based on BLUPs estimated for the complete SAP showed positive associations between all image-derived descriptors and biomass yield (Table 2). The strongest correlation (r = 0.976) was observed between PPH and CHV, indicating that, as expected, the vegetation of taller plants occupies a greater volume. Conversely, PSA was weakly associated with PPW (r = 0.374), which may seem counter-intuitive as plants spreading further into the inter-row space are predicted to have longer leaves, and thus, a greater surface area. While this biological relationship between traits is reflected in their positive but low correlation coefficient, the total plant surface area is more significantly impacted by increases in plant height, as demonstrated by the strong correlation between PPH and PSA (r = 0.908). CHV could be a valuable high-throughput proxy for biomass yield, as demonstrated by its strong correlations with both WB (r = 0.747) and DB (r = 0.787).

Table 1
Phenotypic variation of image-derived descriptors and biomass yield.

Trait	Set	Units	Mean ± SD	Range	H^2
PPH	SAP	mm	1387.42 ± 412.74	645.08-2844.37	0.97
PPW	SAP	mm	525.48 ± 80.04	295.68-765.84	0.73
CHV	SAP	m^3	0.42 ± 0.23	0.07-1.29	0.99
PSA	SAP	m^2	2.03 ± 0.68	0.57-4.57	0.87
WB	SAP	Kg*	19.69 ± 6.99	5.62-63.24	0.85
DB	SAP	Kg*	8.88 ± 3.15	2.23-21.06	0.77
PPH	subset	mm	1633.94 ± 359.82	1218.81-2366.54	
PPW	subset	mm	510.82 ± 58.36	402.08-623.40	
CHV	subset	m^3	0.39 ± 0.11	0.18-0.60	
PSA	subset	m^2	1.40 ± 0.20	1.05-1.73	

PPH – plot-based plant height, PPW – plot-based plant width, CHV – convex-hull volume, PSA – plant surface area, WB – wet biomass, DB – dry biomass.
* Weights taken on a 4.5 m^2 plot.

Table 2
Pearson correlations between all traits (BLUPs) evaluated in the complete SAP.

	PPH	PPW	CHV	PSA	WB	DB
PPH	–	***	***	***	***	***
PPW	0.561	–	***	***	***	***
CHV	0.976	0.634	–	***	***	***
PSA	0.908	0.374	0.897	–	***	***
WB	0.715	0.646	0.747	0.606	–	***
DB	0.748	0.664	0.787	0.676	0.896	–

PPH – plot-based plant height, PPW – plot-based plant width, CHV – convex-hull volume, PSA – plant surface area, WB – wet biomass, DB – dry biomass.
*** Significant at $p < 0.001$.

3.2. Validating image-derived descriptors with ground-truth measurements

To validate their biological significance, the image-derived descriptors PPH, PSA, CHV, and PPW were compared to manually collected ground-truth measurements (Supplementary Table 3). As expected, the highest correlation was observed between PPH and manually measured plant height (r = 0.932) (Fig. 3A), demonstrating the accuracy of this high-throughput trait. PSA was also an accurate descriptor, capturing variation in plant surface area (r = 0.774) (Fig. 3B), in spite of a methodological difference between these two estimated variables. While the ground-truth data were obtained from single plants, PSA was estimated from all plants in the imaged plot, which is reflected in its larger observed phenotypic scale. Interestingly, panicle surface area was the second most highly correlated trait with PSA (r = 0.666) (Supplementary Table 3), which could be attributed to the large variation in panicle size captured in the subset of lines. Note that PI656014, a broomcorn type sorghum, was eliminated for manual surface area measurements, since its unique panicle structure and earlier senescence of lower leaves skewed correlations in this small subset of lines.

Considering that the estimation of PPW was affected by variation in both average leaf length (r = 0.668), and leaf angle (r = 0.516), the derived variable SinAL was calculated to account for both traits simultaneously. The biological significance of PPW could not be better explained by SinAL, because the correlation between these two traits did not improve relative to leaf length alone (r = 0.668) (Fig. 3C). However, PPW had a slightly higher correlation with SinAL than with the average stalk-leaf tip distance (r = 0.603), which defines the canopy length into the inter-row space in a similar manner.

As expected, image-derived CHV was significantly influenced by variation in plant height, demonstrated by its strong correlation with flag leaf height (r = 0.865). However, canopy width is also an important determinant of volume, explaining the relationship evidenced between CHV and average leaf angle (r = 0.545) and SinAL (r = 0.470) (Supplementary Table 3). Plant occupied area was the ground-truth measurement that best correlated with CHV (r = 0.871), slightly higher than flag leaf height, and the closest approximation to the method utilized to extract this feature at the plot level (Fig. 3D).

3.3. Genome-wide association results

Variation in PPH was explained by large genomic intervals located on chromosomes 9 and 6 (Fig. 4A), with the most significant SNPs being *S9_57236791*, *S9_57236778*, *S6_44959724*, and *S6_42736415*. The proportion of the phenotypic variance explained by these associations varied widely ($0.03 < R^2 < 0.339$), and detailed information of all significant polymorphisms is presented in Supplementary Table 4.

A total of 580 SNPs were significantly associated with variation in PPW at a 0.05 FDR threshold (Fig. 4B). These markers had small effects ($0.0744 < R^2 < 0.105$), and were localized to 99 genomic regions across all chromosomes (Table 3). PPW had 67 chromosomal intervals in common with PPH, of which 56 were located on chromosome 6 (Supplementary Table 5). There was one coincident SNP for PPW and PPH on chromosome 9 (*S9_57310782*) at approximately 100Kb from the gene *Dw1*, and eight common regions on chromosome 7, including the marker for *Dw3* (*S7_58610000*). Associations unique for PPW were localized on all chromosomes except 4 and 9, which could represent

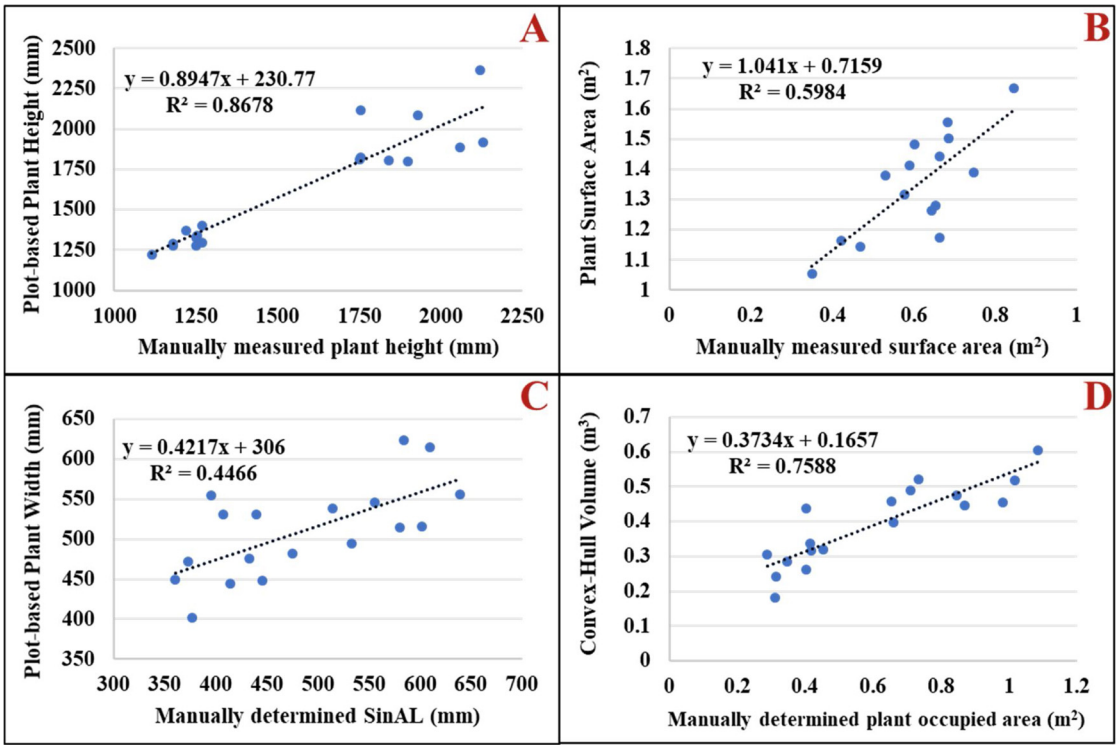

Fig. 3. Ground-truth validation of image-derived descriptors. A. Plot-based plant height and manually measured plant height. B. Plant surface area and manually measured plant surface area. C. Plot-based plant width and manually determined SinAL. D. Convex-hull volume and manually determined plant occupied area.

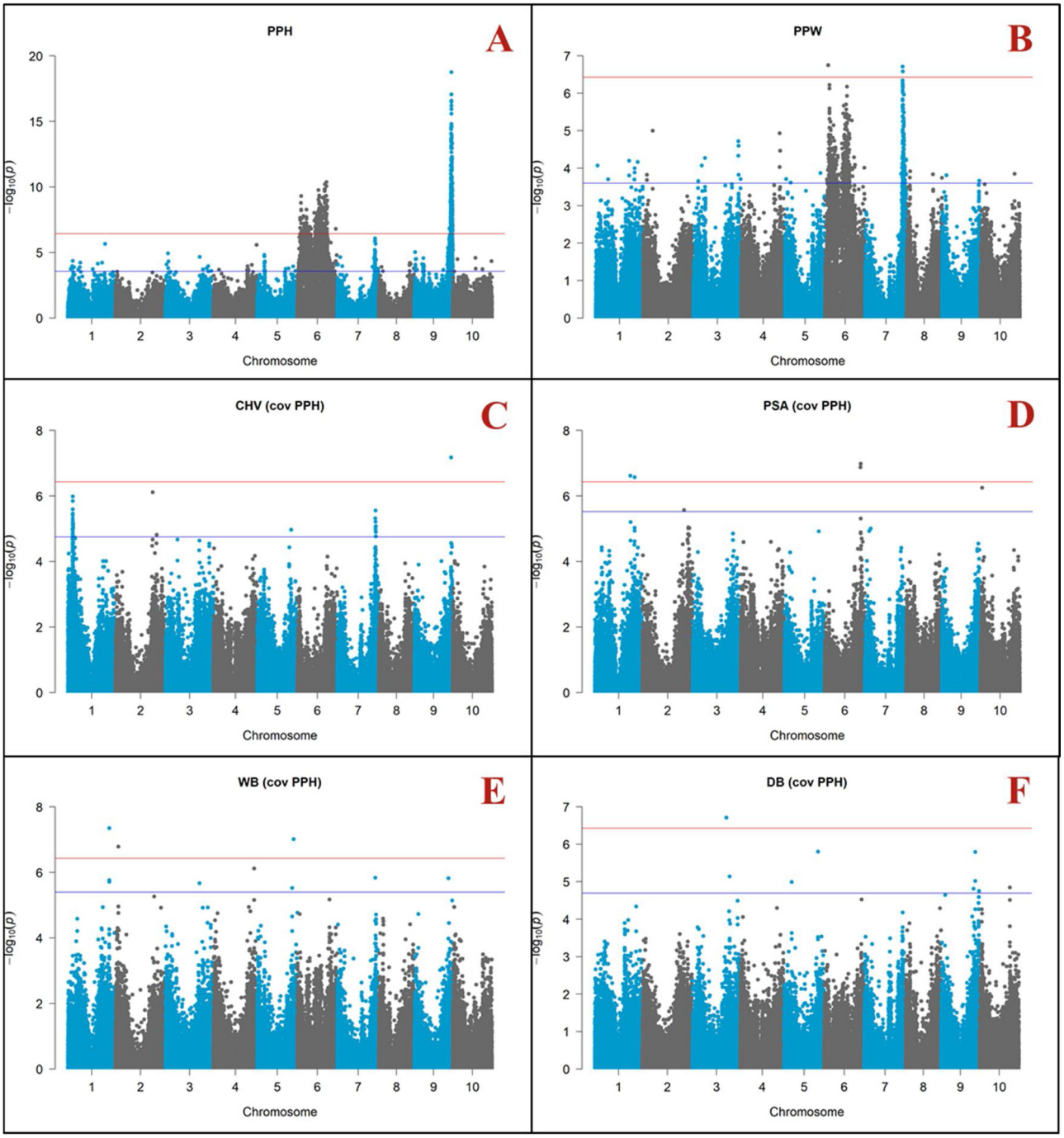

Fig. 4. Manhattan plots, A. Plot-based plant height (PPH), B. Plot-based plant width (PPW), C. Convex-hull volume (CHV) with PPH as covariate, D. Plant surface area (PSA) with PPH as covariate, E. Wet biomass (WB) with PPH as covariate, F. Dry biomass (DB) with PPH as covariate. Horizontal red line indicates Bonferroni significance threshold. Horizontal blue line indicates FDR significance threshold.

genomic regions explaining the ability of plants to grow into the inter-row space.

Considering the strong correlations observed between PPH and CHV, PSA, WB, and DB, BLUPs were estimated for these four traits using two different models, with and without PPH as a covariate. With no covariate, a total of 2697, 1886, 219, and 455 significantly associated SNPs were identified for CHV, PSA, WB, and DB, respectively at a FDR threshold of 0.01 (Fig. S1). These polymorphisms were localized on 173, 186, 53 and 54 chromosomal intervals, respectively (Table 3). Markers for CHV and PSA explained a wide range of the phenotypic variation ($0.004 < R^2 < 0.334$), while the effects of WB and DB-associated SNPs were generally smaller, ranging from 0.056 to 0.144. Due to the strong influence of plant height on these traits, 94%, 86%, 88%, and 96% of their associations coincided with significant SNPs for PPH (Supplementary Table 6). Therefore, the image-derived descriptor PPH was used as a covariate, to facilitate the discovery of novel regions controlling these traits that were not related to plant height. This analysis resulted in the identification of six, twelve, and seven genomic intervals for PSA (cov PPH), CHV (cov PPH), and WB (cov PPH), respectively, at a FDR threshold of 0.05, while DB (cov PPH) had seven associated regions at a FDR of 0.25 (Fig. 4C–F). All markers had similarly small effects with R^2 values ranging from 0.061 to 0.13.

After accounting for plant height variation, the large number of markers in common between PPH and the other image-derived

Table 3
Summary of associated genomic regions for each trait. Number of total significant SNPs per chromosome are in parentheses.

	# Regions[a] (# SNPs)									
Trait	Chr 1	Chr 2	Chr 3	Chr 4	Chr 5	Chr 6	Chr 7	Chr 8	Chr 9	Chr 10
PPH	12 (13)		9 (11)	7 (7)	7 (18)	88 (1740)	16 (57)	6 (12)	28 (1018)	5 (8)
PPW	6 (8)	2 (3)	6 (11)	2 (3)	3 (3)	56 (409)	17 (136)	4 (4)	2 (2)	1 (1)
CHV	13 (17)		6 (8)	8 (11)	6 (13)	85 (1705)	19 (10)	5 (6)	23 (818)	8 (13)
CHV (cov PPH)	4 (32)	2 (2)			1 (1)		4 (8)		1 (1)	
PSA	21 (32)	8 (12)	13 (20)	10 (12)	5 (12)	78 (754)	11 (20)	7 (16)	24 (994)	9 (14)
PSA (cov PPH)	2 (4)	1 (1)				2 (2)				1 (1)
WB	1 (1)	2 (2)	1 (1)	5 (5)	3 (9)	31 (106)	4 (18)		6 (77)	
WB (cov PPH)	1 (3)	1 (1)	1 (1)	1 (1)	2 (2)		1 (1)		1 (1)	
DB				2 (2)	3 (3)	36 (356)	6 (27)	1 (1)	6 (66)	
DB (cov PPH)			2 (2)		2 (2)				2 (4)	1 (2)

PPH – plot-based plant height, PPW – plot-based plant width, CHV – convex-hull volume, PSA – plant surface area, WB – wet biomass, DB – dry biomass. (cov PPH) indicated PPH was used as covariate. [a]Based on average LD decay per chromosome ($r^2 < 0.1$), as reported by Morris et al. (2013).

descriptors were no longer identified, demonstrating the effectiveness of the utilized approach. Only one polymorphism, which corresponds to the tandem duplication of *Dw3 (S7_58610000)* manually scored for the SAP, was associated with both PPH and CHV (cov PPH) (Table 4). Interestingly, this result confirmed the importance of *Dw3* on architectural features in sorghum, particularly leaf angle, which is correlated with CHV (cov PPH). From the 631 SNPs associated with both PPH and DB or WB, none were significant after correcting for PPH. Only three pairs of SNPs in low LD (r^2 = 0.3-0.34) were discovered on chromosomes 9 and 7, which could be explained by the existence of biomass-related genes near *Dw1* and *Dw3* (Table 4).

Interestingly, WB (cov PPH) had at least one SNP in LD or coincidently identified with every trait, including five associations that were initially discovered for WB and remained significant after correcting for plant height (Table 4). These regions in common with PPW, CHV, and PSA, suggest that biomass yield is not only determined by plant height but also the architectural features these descriptors predict, e.g. canopy area and width. Two polymorphisms (*S3_52736967* and *S9_52723997*) were associated with both DB (cov PPH) and WB (cov PPH), suggesting the remaining phenotype-specific markers could be related to biomass yield component traits such as moisture content.

In summary, associations for image-derived descriptors were compared to those for biomass yield to conclude about the ability to predict the genetic determinants of conventionally phenotyped traits. As expected, based on the large variation in plant height observed in this set of accessions, both CHV and PPH had the greatest number of coincident regions with the two biomass traits (DB and WB) (Supplementary Table 5). However, if plant height variation was accounted for (using PPH as a covariate), CHV (cov PPH) was the best image-derived proxy to discover the genetic control of biomass traits (Table 4).

4. Discussion

Image-derived descriptors are novel high-throughput phenotypes that can be used to characterize economically and biologically important features of plants. However, algorithms developed to extract these descriptors, intended to emulate conventional phenotypes, must be validated to confirm they in fact capture the biological feature they seek to describe. In sorghum, plant height has been extensively investigated by manual phenotyping (Brown et al., 2008; Hart et al., 2001; Nagaraja Reddy et al., 2013; Zhao et al., 2016; Zou et al., 2012), making this trait an ideal candidate to characterize and validate our PPH image-derived descriptor. Other sorghum plant architectural features have been research targets with varying degrees of interest. For instance, leaf angle (Hart et al., 2001; Mantilla Perez et al., 2014; Truong et al., 2015; Zhao et al., 2016), leaf length and width (Feltus et al., 2006; Kapanigowda et al., 2014; Sakhi et al., 2013; Shehzad and Okuno et al., 2015; Zou et al., 2012) have been frequently studied but phenotyping has been limited to a single or a few leaves. Leaf area has been poorly characterized at the canopy level (on a maximum of three leaves) (Kapanigowda et al., 2014; Phuong et al., 2013) or only at an early growth stage (Mace et al., 2012). On the contrary, percentage of green leaf area, used to predict stay-green or delayed leaf senescence in sorghum, has received more attention (Haussmann et al., 2002; Rama Reddy et al., 2014; Sabadin et al., 2012; Srinivas et al., 2009). The new image-derived descriptors presented herein, PSA, CHV, and PPW, were developed to capture variation in characteristics such as leaf angle or canopy size on entire plants at the plot-based level, with the goal of discovering their genetic determinants and use them as proxies of biomass yield.

4.1. Comparison of plot-based plant height to previous studies

The PPH parameter was previously presented as proof of concept of the high-throughput phenotyping capacity of PhenoBot 1.0, a novel field-based platform with a side-view design. Image-derived plant height data from the same set of images was obtained using the SGM algorithm (Hirschmuller, 2008), and reported as the Auto-PHe trait by Salas Fernandez et al. (2017). The current study has extracted PPH using a new algorithm, 3DMST (Bao et al., 2018; Li et al., 2017), and has demonstrated improved correlations with ground-truth measurements (ground-truth − 3DMST r = 0.932 as compared to ground-truth–SGM r = 0.824). This completely automated process of stereo matching and feature extraction generated better results than those reported in other HTP attempts to characterize plant height in sorghum. Watanabe et al. (2017) employed a UAV with RGB and NIR-GB cameras and their estimated plant height was only moderately correlated with the manually measured trait (r = 0.518 and r = 0.523, respectively). Pugh et al. (2018) was able to improve the estimation using also UAVs and RGB cameras, reaching a correlation of r = 0.95 when imaging early generation materials from a breeding pipeline, although in advanced materials, the maximum correlation was r = 0.8. While UAVs allow for faster data collection and the use of conventional inter-row spacing, repeatability could be low. It is important to note that, in both studies, altered planting schemes were required to identify plants during image processing. Watanabe et al. (2017) grew five plants per plot with 0.3 m inter-plant spacing, and Pugh et al. (2018) used a 1.22 m alley between plots.

In the complete SAP dataset, the PPH image-derived descriptor was highly correlated with PSA, CHV, WB, and DB (Table 2). The strong correlation observed between plant height and biomass traits was expected based on previous studies (Brenton et al., 2016; Murray et al., 2008). The relationship proved between PPH and PSA indicates that taller plants have more surface area than shorter plants, while the association with CHV demonstrates that, as plants grow taller, they occupy a larger volume by increasing the height of the convex hull.

Table 4
Set of significant SNPs in common between traits, after accounting for variation in plant height.

	CHV (cov PPH)	PSA (cov PPH)	WB (cov PPH)	DB (cov PPH)
PPH	***S7_58610000***		***S9_52723997/S9_52773512 S7_58834007/S7_58834009***	*S9_52723997/S9_52773512*
PPW	***S7_58610000 S7_59170651 S7_59171095 S7_59203187 S7_59648459 S7_59715415 S7_59751825***		***S7_58834007***	
CHV	***S7_58610000 S7_59648459 S7_59715415 S7_59751825***		*S9_52723997/S9_52773512 S7_58834007/S7_58834009*	
PSA		***S6_55505318*** *S1_61607856/ S1_61573809*	*S9_52723997/S9_52773512 S7_58834007/S7_58834009*	*S9_52723997/S9_52773512*
WB	***S7_58610000 S7_59751825***		***S1_64179154 S4_62933630 S5_54086265 S5_56411828 S7_58834007***	
DB	***S7_58610000 S7_59715415 S7_59751825***		***S5_5641182*** *S7_58834007/S7_58834009*	***S5_52633400*** *S5_11726079/ S5_11694646*

Bold indicates marker in common between traits. "marker/marker" refers to significant polymorphisms in linkage disequilibrium ($r^2 > 0.20$) for trait on top and trait on the left, respectively. PPH – plot-based plant height, PPW – plot-based plant width, CHV – convex-hull volume, PSA – plant surface area, WB – wet biomass, DB – dry biomass. Trait followed by (cov PPH) indicates PPH was used as covariate. All marker positions relative to version 1.4 assembly of the sorghum reference genome.

The GWAS for PPH identified the same significant regions on chromosome 6 and 9 previously reported by Salas Fernandez et al. (2017) in which the SGM algorithm was used instead of the 3DMST algorithm (Table 5). The same set of markers was also identified on chromosome 6 and 9 using manually collected data on the SAP (Zhao et al., 2016). These consistent association results between image-derived and manual measurements served as validation of this new high-throughput descriptor. When comparing the two algorithms, it was evident that PPH, obtained with 3DMST, slightly improved the ranking of SNPs on chromosome 6 relative to the Auto-Phe descriptor, in comparison with the manual data. Therefore, both the ground-truth correlations and GWA results demonstrate improvements obtained with the new 3DMST algorithm over the previously reported SGM algorithm.

4.2. Validation of new image-derived descriptors

PSA was highly and positively correlated (r = 0.774) with the manually measured total plant surface area, suggesting the algorithm can accurately recreate the surfaces of plants from the 3D point clouds. Even though slightly higher accuracies have been obtained for leaf area parameters in other studies, the experimental settings are drastically different. In sorghum, high correlations have been found between low-throughput measurements of leaf area (manual or using LI−COR-3100C Area Meter) and foliar areas derived from either RGB images (r = 0.985) (Neilson et al., 2015) or Microsoft Kinect cameras (r = 0.92) (McCormick et al., 2016). In maize, Ge et al. (2016) reported a strong correlation (r = 0.993) between an RGB image-based total plant projected area (pixel count) and leaf area. High precision laser scanners have also been used with success to determine single leaf surface area on individual barley (r = 0.981) (Paulus et al., 2014), maize (r = 0.959), and sorghum plants (r = 0.972) across multiple growth stages (Thapa et al., 2018). However, these high accuracies were achieved by imaging single plants from multiple positions during their vegetative growth phase under controlled conditions. While these technological advances significantly contribute to the development of HTP systems, characterizing densely grown plants under field conditions represents a more challenging scenario for the development of platforms, and the extraction of image-based accurate plant features. In this study, an accurate estimator of plant surface area (PSA) was developed and validated under field conditions at physiological maturity, when canopies are fully developed and overlapping.

The CHV descriptor was validated using the ground-truth variable plant occupied area. While this manually estimated 2D parameter quantifies an area, it is an accurate predictor of vegetative volume since the plot length was maintained constant across images. Volume descriptors have been successfully used to analyze plant growth in barley (Chen et al., 2014; Paulus et al., 2014), and have been identified as one of the best predictors of biomass yield (Chen et al., 2018). In our study, CHV was the trait most highly correlated with both WB and DB (r = 0.747 and r = 0.787, respectively), and thus, it is the best image-derived feature to predict sorghum biomass yield (Table 2). Convex hulls have also been employed to describe traits such as tassel compactness in maize (Gage et al., 2017), root exploration in rice (Iyer-pascuzzi et al., 2010; Topp et al., 2013), tomato (Tracy et al., 2012), and maize (Zurek et al., 2015), and shoot architecture/compactness in sorghum (McCormick et al., 2016; Neilson et al., 2015), tomato, and tobacco (Conn et al., 2017). These studies confirmed the important role that CHV can play in analyzing not only overall yield, but also plant compactness and growth throughout the growing cycle. Even though data are only presented herein from the set of images collected at the end of the season, future work will include the analysis of images obtained throughout the growing period to determine the accuracy of CHV as an indicator of sorghum growth under field conditions.

Based on the validation dataset, the PPW parameter had an intermediate and positive correlation with SinAL, which is a function of both leaf length and leaf angle. SinAL describes how far the plant grows into

Table 5
Comparison of GWAS results using different phenotyping methods.

	PPH			Auto-Phe[a]			Manual[b]		
SNP[c]	- LOG10 (P)	R^2	Rank[d]	- LOG10 (P)	R^2	Rank[d]	- LOG10 (P)	R^2	Rank[d]
S9_57236791	18.764	0.293	1	18.673	0.301	1	17.903	0.292	2
S9_57236778	17.065	0.274	2	17.634	0.283	2	18.421	0.29	1
S6_44959724	10.383	0.147	1	10.427	0.155	1	10.102	0.159	8
S6_42736415	10.202	0.152	2	9.795	0.153	4	10.742	0.18	2
S6_39106643	9.19	0.147	15	8.308	0.135	27	11.112	0.202	1

[a] Descriptor developed using the SGM algorithm on the same set of images as published by (Salas-Fernandez et al. (2017).
[b] Data collected manually in 2010 and published by Zhao et al. (2016).
[c] All marker positions relative to version 1.4 assembly of the sorghum reference genome.
[d] Marker ranking is based on P-values.

the interrow space, i.e., the width of the plant perpendicular to the planting direction. Longer leaves clearly spread further into the interrow space than shorter leaves, while the angle with which the leaf expands also determines the canopy extent. Paulus et al. (2014) reported a high correlation (r = 0.927) between a laser-based and conventionally measured plant width on a single barley plant under controlled conditions. While PPW had a lower accuracy, it was collected from a dense canopy on plants in an uncontrolled environment.

4.3. GWA results for new image-derived descriptors

Considering the significant correlations between PPH and the other image-derived descriptors, the association analysis for PSA, CHV, WB, and DB resulted in the identification of genetic regions known to control plant height (Supplementary Table 6, Fig. S1). Therefore, PPH was used as a covariate in the estimation of BLUPs for all four traits (Fig. 4C–F).

The significant markers on chromosomes 1, 6 and 10 associated with variation in PSA (cov PPH) overlapped with regions controlling tiller number, based on previous studies (Feltus et al., 2006; Hart et al., 2001; Kong et al., 2014; Mocoeur et al., 2015; Shiringani et al., 2010) (Supplementary Table 5). These coincident genetic determinants for the two traits are explained by the greater surface area observed in plants with more tillers. The effectiveness of PSA (cov PPH) to capture variation in canopy surface was demonstrated by the validated significant regions on chromosomes 1, 2 (Haussmann et al., 2002; Srinivas et al., 2009), and 10 (McCormick et al., 2016) that harbor QTL previously reported for green/leaf area. As indicated by our ground-truth validation, PSA also captured variability in surface area attributed to differences in stem sizes, demonstrated by the common QTL on chromosome 10 identified in our study and the HTP research by McCormick et al. (2016). Finally, our results confirm that these image-derived descriptors can facilitate the discovery of novel (not previously reported) regions controlling architectural or biomass yield QTL, such as the four markers (*S2_68681642, S5_60278659, S6_334778,* and *S7_654918*) associated with PSA that should be further validated.

The shoot compactness trait reported by McCormick et al. (2016) was measured using a convex hull surface area, which is similar to the CHV descriptor presented herein, since both variables are based on the fit of a convex hull around a sorghum plant. Therefore, three of the four genomic regions discovered for CHV (cov PPH) on chromosome 7 were also identified by McCormick et al. (2016) for shoot compactness. The size of the convex hull can be impacted by variations in leaf angle, as demonstrated by the strong correlation observed between the two traits in our ground-truth validation data set (r = 0.545) (Supplementary Table 3). This relationship between our image-derived descriptor (CHV (cov PPH)) and the conventional trait (leaf angle) was confirmed by the chromosome 1 and 7 regions discovered in common between our study and previous reports (Hart et al., 2001; Truong et al., 2015; McCormick et al., 2016; Zhao et al., 2016) (Supplementary Table 5). Since the number of tillers can impact the size of the convex hull, the co-localization of significant regions for CHV (cov PPH) and previously reported QTL for tiller number was expected and corroborated for 41% of the associations (Supplementary Table 5). These outcomes support our validation results, demonstrating that CHV describes plant compactness, canopy architecture and simpler traits, such as leaf angle and tiller number. The value of CHV (cov PPH) as a proxy for biomass yield is demonstrated not only by the coincident associations between the image-derived trait and our own biomass traits (Table 4), but also by the large number of coincident QTL with previous studies characterizing fresh and dry total biomass, fresh and dry shoot weight and dry leaf weight (Felderhoff et al., 2012; Gelli et al., 2016; Guan et al., 2011; Kapanigowda et al., 2014; Mace et al., 2012; Mocoeur et al., 2015; Murray et al., 2008; Spagnolli et al., 2016; Wang et al., 2014, 2016; Zhang et al., 2015). Finally, two markers explaining variation in CHV (*S7_654918*) and CHV (cov PPH) (*S2_57764975*) are novel discoveries not previously reported for either architectural traits or biomass yield, and should be further validated for future use.

The GWAS for PPW produced a large number of significant SNPs at a 0.05 FDR threshold. Since the biological significance of this parameter encompasses multiple conventional traits, the SNPs identified for PPW could be associated with different plant architectural features. For instance, 86 of the 99 significant regions for PPW co-localized with conventionally phenotyped tiller number QTL (Alam et al., 2014; Feltus et al., 2006; Hart et al., 2001; Kong et al., 2014; Mocoeur et al., 2015; Paterson et al., 1995; Shehzad and Okuno, 2015; Shiringani et al., 2010; Takai et al., 2012; Upadhyaya et al., 2012; Zhang et al., 2015; Zhao et al., 2016; Zou et al., 2012) (Supplementary Table 5). Even though tiller number was not recorded in this study, a wider canopy area would be expected for accessions with more tillers growing into the interrow space. PPW-associated regions on chromosomes 1, 4, 6, 7, 8, and 9 are within previously identified QTL for leaf length (Feltus et al., 2006; Kapanigowda et al., 2014; McCormick et al., 2016; Shehzad and Okuno, 2015) (Supplementary Table 5). These results and the strong correlation with average leaf length (r = 0.668) (Supplementary Table 3), suggests that this descriptor can capture variability in leaf length and be used to dissect its genetic architecture.

Leaf angle, one of the components of SinAL, is an architectural trait of increased interest in sorghum. The PPW-significant regions on chromosome 7 and 6 were likely discovered due to the genetic leaf angle determinants, such as *DW3*, physically located in these intervals, as reported by several groups (Hart et al., 2001; McCormick et al., 2016; Zhao et al., 2016). Other regions in common between PPW and known leaf angle QTL confirm the important effect of this trait on canopy width determination, including SNP *S3_7490326* (Mantilla Perez et al., 2014; McCormick et al., 2016), *S1_19054010* (Hart et al., 2001), *S3_17831835* and two regions between *S1_60074351* and *S1_60178175* (Truong et al., 2015). However, other leaf angle controlling intervals on chromosomes 1, 2, 3, 4, 5, 6 and 9 (Mantilla Perez et al., 2014; McCormick et al., 2016; Truong et al., 2015; Zhao et al., 2016), were

not verified in this study. The lack of consistent results in these positions could be attributed to methodological differences between studies, since PPW describes width variation in the entire canopy at the end of the season, not only determined by angle changes, while individual early or late leaves (e.g. leaf 3, 5, pre-flag leaf) were previously characterized. The significant region on chromosome 7 contains the sorghum gene *Dwarf3* (Multani et al., 2003), which is not only a major height gene in sorghum, but also a determinant of leaf angle (Truong et al., 2015). It has been speculated that another leaf angle gene is located in this region near *Dw3* (Zhao et al., 2016), and this was further supported by Truong et al. (2015), who reported a QTL in the same region using a RIL population that did not segregate for *Dw3* (both parents R07018 and R07020 carried the *Dw3* allele). Similarly to what we observed for other image-derived descriptors, there were novel intervals on chromosome 2 and 5 for PPW that have not been previously associated with traditionally measured canopy traits, and could be attributed to variation in parameters uniquely exposed by the new HTP features.

5. Conclusions

In summary, we have implemented and verified a new algorithm for the completely automated extraction of new image-derived plant architectural parameters. This new algorithm resulted in an improved correlation between PPH and ground-truth measurements, while continuing to detect genomic regions known to control plant height in sorghum. The PSA descriptor was validated by both its correlation with manually measured parameters, and the associated regions in common with previous reports. CHV and PPW are novel and complex features determined by numerous traditionally measured traits. The relationship between CHV and plant compactness, or between PPW and both leaf angle and length, provide innovative ways to characterize plant architecture at large scale under field conditions. Our data demonstrate that biomass yields can be predicted by the CHV descriptor, suggesting it could be utilized as a novel tool for phenotyping, selection and breeding biomass sorghum. While the GWA results for these new parameters facilitated the discovery of genomic regions in common with previously reported plant characteristics, they also included a set of novel polymorphisms/QTL. After validation, these genomic regions could represent new resources for the genetic improvement of architectural features, and subsequently yield, in sorghum breeding programs.

Acknowledgements

This work was supported by the National Institute of Food and Agriculture, United States Department of Agriculture (grant number 2012-67009-19713); and the Plant Sciences Institute at Iowa State University. MGSF was also supported by the United States Department of Agriculture, National Institute of Food and Agriculture (grant number IOW04314).

We thank Lisa Coffey (Schnable Lab) and Nicole Lindsey (Salas Fernandez Lab) for their assistance designing and conducting the sorghum field experiments. We also acknowledge Patrick Rasmussen and Dylan Shah for their contributions to retrofitting the tractor; Gregory Schoenbaum, Hang Lu, Jingyao Gai, Kimberly McFee, Maureen Booth, Kenneth Linkenmeyer, Elijah McKeever, Megan Mullen, Nur Husna Izzati Shafeai, and Tara Simon for maintaining field plots and the collection of ground-truth data. We finally recognize Joshua Kemp and Ezequiel Delfino for their assistance during ground-truth validation.

Appendix A. Supplementary data

Supplementary material related to this article can be found, in the online version, at doi:https://doi.org/10.1016/j.fcr.2019.107619.

References

Alam, M.M., Mace, E.S., van Oosterom, E.J., Cruickshank, A., Hunt, C.H., Hammer, G.L., Jordan, D.R., 2014. QTL analysis in multiple sorghum populations facilitates the dissection of the genetic and physiological control of tillering. Theor. Appl. Genet. 127, 2253–2266. https://doi.org/10.1007/s00122-014-2377-9.

Andrade-Sanchez, P., Gore, M.A., Heun, J.T., Thorp, K.R., Carmo-Silva, A.E., French, A.N., Salvucci, M.E., White, J.W., 2014. Development and evaluation of a field-based high-throughput phenotyping platform. Funct. Plant Biol. 41, 68–79. https://doi.org/10.1071/FP13126.

Austin, R.B., Ford, M.A., Edrich, J.A., Hooper, B.E., 1976. Some effects of leaf posture on photosynthesis and yield in wheat. Ann. Appl. Biol. 83, 425–446. https://doi.org/10.1017/S0021859600037680.

Bai, G., Ge, Y., Hussain, W., Baenziger, P.S., Graef, G., 2016. A multi-sensor system for high throughput field phenotyping in soybean and wheat breeding. Comput. Electron. Agric. 128, 181–192. https://doi.org/10.1016/j.compag.2016.08.021.

Bao, Y., Tang, L., Breitzman, M.W., Salas Fernandez, M.G., Schnable, P.S., 2018. Field - based robotic phenotyping of sorghum plant architecture using stereo vision. J. F. Robot. https://doi.org/10.1002/rob.21830.

Bradbury, P.J., Zhang, Z., Kroon, D.E., Casstevens, T.M., Ramdoss, Y., Buckler, E.S., 2007. TASSEL: software for association mapping of complex traits in diverse samples. Bioinformatics 23, 2633–2635. https://doi.org/10.1093/bioinformatics/btm308.

Brenton, Z.W., Cooper, E.A., Myers, M.T., Boyles, R.E., Shakoor, N., Zielinski, K.J., Rauh, B.L., Bridges, W.C., Morris, G.P., Kresovich, S., 2016. A genomic resource for the development, improvement, and exploitation of sorghum for bioenergy. Genetics 204, 21–33. https://doi.org/10.1534/genetics.115.183947.

Brown, P.J., Rooney, W.L., Franks, C., Kresovich, S., 2008. Efficient mapping of plant height quantitative trait loci in a sorghum association population with introgressed dwarfing genes. Genetics 180, 629–637. https://doi.org/10.1534/genetics.108.092239.

Busemeyer, L., Mentrup, D., Möller, K., Wunder, E., Alheit, K., Hahn, V., Maurer, H.P., Reif, J.C., Würschum, T., Müller, J., Rahe, F., Ruckelshausen, A., 2013. Breedvision - A multi-sensor platform for non-destructive field-based phenotyping in plant breeding. Sensors (Switzerland) 13, 2830–2847. https://doi.org/10.3390/s130302830.

Casa, A.M., Pressoir, G., Brown, P.J., Mitchell, S.E., Rooney, W.L., Tuinstra, M.R., Franks, C.D., Kresovich, S., 2008. Community resources and strategies for association mapping in Sorghum. Crop Sci. 48, 30–40. https://doi.org/10.2135/cropsci2007.02.0080.

Chen, D., Neumann, K., Friedel, S., Kilian, B., Chen, M., Altmann, T., Klukas, C., 2014. Dissecting the phenotypic components of crop plant growth and drought responses based on high-throughput image analysis. Plant Cell Online 26, 4636–4655. https://doi.org/10.1105/tpc.114.129601.

Chen, D., Shi, R., Pape, J.M., Neumann, K., Arend, D., Graner, A., Chen, M., Klukas, C., 2018. Predicting plant biomass accumulation from image-derived parameters. Gigascience 7, 1–13. https://doi.org/10.1093/gigascience/giy001.

Comar, A., Burger, P., De Solan, B., Baret, F., Daumard, F., Hanocq, J.F., 2012. A semi-automatic system for high throughput phenotyping wheat cultivars in-field conditions: description and first results. Funct. Plant Biol. 39, 914–924. https://doi.org/10.1071/FP12065.

Conn, A., Pedmale, U.V., Chory, J., Stevens, C.F., Navlakha, S., 2017. A statistical description of plant shoot architecture. Curr. Biol. 27, 2078–2088. https://doi.org/10.1016/j.cub.2017.06.009. e3.

Crain, J.L., Wei, Y., Barker, J., Thompson, S.M., Alderman, P.D., Reynolds, M., Zhang, N., Poland, J., 2016. Development and deployment of a portable field phenotyping platform. Crop Sci. 56, 965–975. https://doi.org/10.2135/cropsci2015.05.0290.

Duggal, P., Gillanders, E.M., Holmes, T.N., Bailey-Wilson, J.E., 2008. Establishing an adjusted p-value threshold to control the family-wide type 1 error in genome wide association studies. BMC Genomics 9, 1–8. https://doi.org/10.1186/1471-2164-9-516.

Felderhoff, T.J., Murray, S.C., Klein, P.E., Sharma, A., Hamblin, M.T., Kresovich, S., Vermerris, W., Rooney, W.L., 2012. QTLs for energy-related traits in a sweet × grain sorghum [Sorghum bicolor (L.) Moench] mapping population. Crop Sci. 52, 2040–2049. https://doi.org/10.2135/cropsci2011.11.0618.

Feltus, F.A., Hart, G.E., Schertz, K.F., Casa, A.M., Kresovich, S., Abraham, S., Klein, P.E., Brown, P.J., Paterson, A.H., 2006. Alignment of genetic maps and QTLs between inter- and intra-specific sorghum populations. Theor. Appl. Genet. 112, 1295–1305. https://doi.org/10.1007/s00122-006-0232-3.

Furbank, R.T., Tester, M., 2011. Phenomics - technologies to relieve the phenotyping bottleneck. Trends Plant Sci. 16, 635–644. https://doi.org/10.1016/j.tplants.2011.09.005.

Gage, J.L., Miller, N.D., Spalding, E.P., Kaeppler, S.M., de Leon, N., 2017. TIPS: a system for automated image-based phenotyping of maize tassels. Plant Methods 13, 1–12. https://doi.org/10.1186/s13007-017-0172-8.

Ge, Y., Bai, G., Stoerger, V., Schnable, J.C., 2016. Temporal dynamics of maize plant growth, water use, and leaf water content using automated high throughput RGB and hyperspectral imaging. Comput. Electron. Agric. 127, 625–632. https://doi.org/10.1016/j.compag.2016.07.028.

Gelli, M., Mitchell, S.E., Liu, K., Clemente, T.E., Weeks, D.P., Zhang, C., Holding, D.R., Dweikat, I.M., 2016. Mapping QTLs and association of differentially expressed gene transcripts for multiple agronomic traits under different nitrogen levels in sorghum. BMC Plant Biol. 16. https://doi.org/10.1186/s12870-015-0696-x.

Großkinsky, D.K., Svensgaard, J., Christensen, S., Roitsch, T., 2015. Plant phenomics and the need for physiological phenotyping across scales to narrow the genotype-to-phenotype knowledge gap. J. Exp. Bot. 66, 5429–5440. https://doi.org/10.1093/jxb/

erv345.
Guan, Y.an, Wang, Hailian, Qin, L., Zhang, Hwen, Yang, Ybing, Gao, Fju, Li, Ryu, gang, Wang Hong, 2011. QTL mapping of bio-energy related traits in Sorghum. Euphytica 182, 431–440. https://doi.org/10.1007/s10681-011-0528-5.
Guo, W., Zheng, B., Potgieter, A.B., Diot, J., Watanabe, K., Noshita, K., Jordan, D.R., Wang, X., Watson, J., Ninomiya, S., Chapman, S.C., 2018. Aerial imagery analysis – quantifying appearance and number of Sorghum Heads for applications in breeding and agronomy. Front. Plant Sci. 9, 1–9. https://doi.org/10.3389/fpls.2018.01544.
Hart, G.E., Schertz, K.F., Peng, Y., Syed, N.H., 2001. Genetic mapping of Sorghum bicolor (L.) Moench QTLs that control variation in tillering and other morphological characters. Theor. Appl. Genet. 103, 1232–1242. https://doi.org/10.1007/s001220100582.
Haussmann, B.I.G., Mahalakshmi, V., Reddy, B.V.S., Seetharama, N., Hash, C.T., Geiger, H.H., 2002. QTL mapping of stay-green in two sorghum recombinant inbred populations. Theor. Appl. Genet. 106, 133–142. https://doi.org/10.1007/s00122-002-1012-3.
Hirschmuller, H., 2008. Stereo processing by semiglobal matching and mutual information. IEEE Trans. Pattern Anal. Mach. Intell. 30, 328–341. https://doi.org/10.1109/TPAMI.2007.1166.
Hu, P., Chapman, S.C., Wang, X., Potgieter, A., Duan, T., Jordan, D., Guo, Y., Zheng, B., 2018. Estimation of plant height using a high throughput phenotyping platform based on unmanned aerial vehicle and self-calibration: example for sorghum breeding. Eur. J. Agron. 95, 24–32. https://doi.org/10.1016/j.eja.2018.02.004.
Iyer-pascuzzi, A.S., Symonova, O., Mileyko, Y., Hao, Y., Belcher, H., Harer, J., Weitz, J.S., Benfey, P.N., 2010. Imaging and analysis platform for automatic phenotyping and trait ranking of plant system. Plant Physiol. 152, 1148–1157. https://doi.org/10.1104/pp.109.150748.
Kapanigowda, M.H., Payne, W.A., Rooney, W.L., Mullet, J.E., Balota, M., 2014. Quantitative trait locus mapping of the transpiration ratio related to preflowering drought tolerance in sorghum (Sorghum bicolor). Funct. Plant Biol. 41, 1049–1065. https://doi.org/10.1071/FP13363.
Kong, W., Guo, H., Goff, V.H., Lee, T.H., Kim, C., Paterson, A.H., 2014. Genetic analysis of vegetative branching in sorghum. Theor. Appl. Genet. 127, 2387–2403. https://doi.org/10.1007/s00122-014-2384-x.
Lee, E.A., Tollenaar, M., 2007. Physiological basis of successful breeding strategies for maize grain yield. Crop Sci. 47, S202–S215. https://doi.org/10.2135/cropsci2007.04.0010IPBS.
Li, L., Yu, X., Zhang, S., Zhao, X., Zhang, L., 2017. 3D cost aggregation with multiple minimum spanning trees for stereo matching. Appl. Opt. 56, 3411–3420. https://doi.org/10.1364/AO.56.003411.
Mace, E., Innes, D., Hunt, C., Wang, X., Tao, Y., Baxter, J., Hassall, M., Hathorn, A., Jordan, D., 2019. The Sorghum QTL Atlas: a powerful tool for trait dissection, comparative genomics and crop improvement. Theor. Appl. Genet. 132, 751–766. https://doi.org/10.1007/s00122-018-3212-5.
Mace, E.S., Singh, V., van Oosterom, E.J., Hammer, G.L., Hunt, C.H., Jordan, D.R., 2012. QTL for nodal root angle in sorghum (Sorghum bicolor L. Moench) co-locate with QTL for traits associated with drought adaptation. Theor. Appl. Genet. 124, 97–109. https://doi.org/10.1007/s00122-011-1690-9.
Mantilla-Perez, M.B., Salas Fernandez, M.G., 2017. Differential manipulation of leaf angle throughout the canopy: current status and prospects. J. Exp. Bot. 68, 5699–5717. https://doi.org/10.1093/jxb/erx378.
Mantilla Perez, M.B., Zhao, J., Yin, Y., Hu, J., Salas Fernandez, M.G., 2014. Association mapping of brassinosteroid candidate genes and plant architecture in a diverse panel of Sorghum bicolor. Theor. Appl. Genet. 127, 2645–2662. https://doi.org/10.1007/s00122-014-2405-9.
McCormick, R.F., Truong, S.K., Mullet, J.E., 2016. 3D sorghum reconstructions from depth images identify QTL regulating shoot architecture. Plant Physiol. 172, 823–834. https://doi.org/10.1104/pp.16.00948.
Mocoeur, A., Zhang, Y.M., Liu, Z.Q., Shen, X., Zhang, L.M., Rasmussen, S.K., Jing, H.C., 2015. Stability and genetic control of morphological, biomass and biofuel traits under temperate maritime and continental conditions in sweet sorghum (Sorghum bicolour). Theor. Appl. Genet. 128, 1685–1701. https://doi.org/10.1007/s00122-015-2538-5.
Morinaka, Y., Sakamoto, T., Inukai, Y., Agetsuma, M., Kitano, H., Ashikari, M., Matsuoka, M., 2006. Morphological alteration caused by brassinosteroid insensitivity increases the biomass and grain production of rice. Plant Physiol. 141, 924–931. https://doi.org/10.1104/pp.106.077081.
Morris, G.P., Ramu, P., Deshpande, S.P., Hash, C.T., Shah, T., Upadhyaya, H.D., Riera-Lizarazu, O., Brown, P.J., Acharya, C.B., Mitchell, S.E., Harriman, J., Glaubitz, J.C., Buckler, E.S., Kresovich, S., 2013. Population genomic and genome-wide association studies of agroclimatic traits in sorghum. Proc. Natl. Acad. Sci. 110, 453–458. https://doi.org/10.1073/pnas.1215985110.
Mueller-Sim, T., Jenkins, M., Abel, J., Kantor, G., 2017. The Robotanist: a ground-based agricultural robot for high-throughput crop phenotyping. Proc. - IEEE Int. Conf. Robot. Autom. 3634–3639. https://doi.org/10.1109/ICRA.2017.7989418.
Mullet, J., Morishige, D., McCormick, R., Truong, S., Hilley, J., McKinley, B., Anderson, R., Olson, S.N., Rooney, W., 2014. Energy sorghum - A genetic model for the design of C4 grass bioenergy crops. J. Exp. Bot. 65, 3479–3489. https://doi.org/10.1093/jxb/eru229.
Mullet, J.E., 2017. High-biomass C4grasses—filling the yield gap. Plant Sci. 261, 10–17. https://doi.org/10.1016/j.plantsci.2017.05.003.
Multani, D.S., Briggs, S.P., Chamberlin, M.A., Blakeslee, J.J., Murphy, A.S., Johal, G.S., 2003. Loss of an MDR transporter in compact stalks of maize br2 and sorghum dw3 mutants. Science 302, 81–84. https://doi.org/10.1126/science.1086072.
Murray, S.C., Rooney, W.L., Mitchell, S.E., Sharma, A., Klein, P.E., Mullet, J.E., Kresovich, S., 2008. Genetic improvement of sorghum as a biofuel feedstock: II. QTL for stem and leaf structural carbohydrates. Crop Sci. 48, 2180–2193. https://doi.org/10.2135/cropsci2008.01.0068.
Nagaraja Reddy, R., Madhusudhana, R., Murali Mohan, S., Chakravarthi, D.V.N., Mehtre, S.P., Seetharama, N., Patil, J.V., 2013. Mapping QTL for grain yield and other agronomic traits in post-rainy sorghum [Sorghum bicolor (L.) Moench]. Theor. Appl. Genet. 126, 1921–1939. https://doi.org/10.1007/s00122-013-2107-8.
Neilson, E.H., Edwards, A.M., Blomstedt, C.K., Berger, B., Møller, B.L., Gleadow, R.M., 2015. Utilization of a high-throughput shoot imaging system to examine the dynamic phenotypic responses of a C4 cereal crop plant to nitrogen and water deficiency over time. J. Exp. Bot. 66, 1817–1832. https://doi.org/10.1093/jxb/eru526.
Olson, S.N., Ritter, K., Rooney, W., Kemanian, A., McCarl, B.A., Zhang, Y., Hall, S., Packer, D., Mullet, J., 2012. High biomass yield energy sorghum: developing a genetic model for C4 grass bioenergy crops. Biofuels, Bioprod. Biorefining 6, 640–655. https://doi.org/10.1002/bbb.1357.
Ortiz, D., Hu, J., Salas Fernandez, M.G., 2017. Genetic architecture of photosynthesis in Sorghum bicolor under non-stress and cold stress conditions. J. Exp. Bot. 68, 4545–4557. https://doi.org/10.1093/jxb/erx276.
Parry, M.A.J., Reynolds, M., Salvucci, M.E., Raines, C., Andralojc, P.J., Zhu, X.-G., Price, G.D., Condon, A.G., Furbank, R.T., 2011. Raising yield potential of wheat. II. Increasing photosynthetic capacity and efficiency. J. Exp. Bot. 62, 453–467. https://doi.org/10.1093/jxb/erq304.
Paterson, A.H., Schertz, K.F., Lin, Y.-R., Liu, S.-C., Chang, Y.-L., 1995. The weediness of wild plants: molecular analysis of genes influencing dispersal and persistence of johnsongrass, Sorghum halepense (L.) Pers (Poaceae/rhizomes/genome mapping/biotechnology risk assessment/plant growth regulation). Agric. Sci. 92, 6127–6131.
Pauli, D., Andrade-Sanchez, P., Carmo-Silva, A.E., Gazave, E., French, A.N., Heun, J., Hunsaker, D.J., Lipka, A.E., Setter, T.L., Strand, R.J., Thorp, K.R., Wang, S., White, J.W., Gore, M.A., 2016. Field-based high-throughput plant phenotyping reveals the temporal patterns of quantitative trait loci associated with stress-responsive traits in cotton. G3: Genes, Geromes, Genetics 6, 865–879. https://doi.org/10.1534/g3.115.023515.
Paulus, S., Schumann, H., Kuhlmann, H., Léon, J., 2014. High-precision laser scanning system for capturing 3D plant architecture and analysing growth of cereal plants. Biosyst. Eng. 121, 1–11. https://doi.org/10.1016/j.biosystemseng.2014.01.010.
Pendleton, J.W., Smith, G.E., Winter, S.R., Johnston, T.J., 1968. Field investigations of the relationships of leaf angle in corn (Zea mays L.) to grain yield and apparent photosynthesis. Agron. J. 60, 422–424. https://doi.org/10.2134/agronj1968.00021962006000040027x.
Phuong, N., Stützel, H., Uptmoor, R., 2013. Quantitative trait loci associated to agronomic traits and yield components in a &i&Sorghum bicolor&/i& L. Moench RIL population cultivated under pre-flowering drought and well-watered conditions. Agric. Sci. 04, 781–791. https://doi.org/10.4236/as.2013.412107.
Poorter, H., Fiorani, F., Pieruschka, R., Putten, W.H., Van Der Kleyer, M., Schurr, U., 2016. Pampered inside, pestered outside? Differences and similarities between plants growing in controlled conditions and in the field. New Phytol. 212, 838–855. https://doi.org/10.1111/nph.14243.
Potgieter, A.B., George-Jaeggli, B., Chapman, S.C., Laws, K., Suárez Cadavid, L.A., Wixted, J., Watson, J., Eldridge, M., Jordan, D.R., Hammer, G.L., 2017. Multi-spectral imaging from an unmanned aerial vehicle enables the assessment of seasonal leaf area dynamics of Sorghum breeding lines. Front. Plant Sci. 8, 1–11. https://doi.org/10.3389/fpls.2017.01532.
Pugh, N.A., Horne, D.W., Murray, S.C., Carvalho, G., Malambo, L., Jung, J., Chang, A., Maeda, M., Popescu, S., Chu, T., Starek, M.J., Brewer, M.J., Richardson, G., Rooney, W.L., 2018. Temporal estimates of crop growth in sorghum and maize breeding enabled by unmanned aerial systems. Plant Phenome J. 1, 1–10. https://doi.org/10.2135/tppj2017.08.0006.
R_Core_Development_Team, 2013. R: a Language and Environment for Statistical Computing.
Rahaman, M.M., Chen, D., Gillani, Z., Klukas, C., Chen, M., 2015. Advanced phenotyping and phenotype data analysis for the study of plant growth and development. Front. Plant Sci. 6, 1–15. https://doi.org/10.3389/fpls.2015.00619.
Rama Reddy, N.R., Ragimasalawada, M., Sabbavarapu, M.M., Nadoor, S., Patil, J.V., 2014. Detection and validation of stay-green QTL in post-rainy sorghum involving widely adapted cultivar, M35-1 and a popular stay-green genotype B35. BMC Genomics 15. https://doi.org/10.1186/1471-2164-15-909.
Sabadin, P.K., Malosetti, M., Boer, M.P., Tardin, F.D., Santos, F.G., Guimarães, C.T., Gomide, R.L., Andrade, C.L.T., Albuquerque, P.E.P., Caniato, F.F., Mollinari, M., Margarido, G.R.A., Oliveira, B.F., Schaffert, R.E., Garcia, A.A.F., van Eeuwijk, F.A., Magalhaes, J.V., 2012. Studying the genetic basis of drought tolerance in sorghum by managed stress trials and adjustments for phenological and plant height differences. Theor. Appl. Genet. 124, 1389–1402. https://doi.org/10.1007/s00122-012-1795-9.
Sakhi, S., Shehzad, T., Rehman, S., Okuno, K., 2013. Mapping the QTLs underlying drought stress at developmental stage of sorghum (Sorghum bicolor (L.) Moench) by association analysis. Euphytica 193, 433–450. https://doi.org/10.1007/s10681-013-0963-6.
Salas Fernandez, M.G., Bao, Y., Tang, L., Schnable, P.S., 2017. A high-throughput, field-based phenotyping technology for tall biomass crops. Plant Physiol. 174, 2008–2022. https://doi.org/10.1104/pp.17.00707.
SAS Institute, 2008. SAS/STAT 9.2: User's Guide. SAS Inst. Inc., Cary, NC.
Shehzad, T., Okuno, K., 2015. QTL mapping for yield and yield-contributing traits in sorghum (Sorghum bicolor (L.) Moench) with genome-based SSR markers. Euphytica 203, 17–31. https://doi.org/10.1007/s10681-014-1243-9.
Shiringani, A.L., Frisch, M., Friedt, W., 2010. Genetic mapping of QTLs for sugar-related traits in a RIL population of Sorghum bicolor L. Moench. Theor. Appl. Genet. 121, 323–336. https://doi.org/10.1007/s00122-010-1312-ySinclair.
Sinclair, T.R., Sheehy, J.E., 1999. Erect leaves and photosynthesis in rice. Science 283,

1456–1457. https://doi.org/10.1126/science.283.5407.1455c.
Sodhi, P., Vijayarangan, S., Wettergreen, D.S., 2017. In-field segmentation and identification of plant structures using 3D imaging. IEEE/RSJ Int. Conf. Intell. Robot. Syst. https://doi.org/10.1109/IROS.2017.8206407.
Spagnolli, F.C., Mace, E., Jordan, D., Borrás, L., Gambin, B.L., 2016. Quantitative trait loci of plant attributes related to sorghum grain number determination. Crop Sci. 56, 3046–3054. https://doi.org/10.2135/cropsci2016.03.0185.
Srinivas, G., Satish, K., Madhusudhana, R., Nagaraja Reddy, R., Murali Mohan, S., Seetharama, N., 2009. Identification of quantitative trait loci for agronomically important traits and their association with genic-microsatellite markers in sorghum. Theor. Appl. Genet. 118, 1439–1454. https://doi.org/10.1007/s00122-009-0993-6.
Storey, J.D., Tibshirani, R., 2003. Statistical significance for genomewide studies. Proc. Natl. Acad. Sci. 100, 9440–9445. https://doi.org/10.1073/pnas.1530509100.
Takai, T., Yonemaru, Jichi, Kaidai, H., Kasuga, S., 2012. Quantitative trait locus analysis for days-to-heading and morphological traits in an RIL population derived from an extremely late flowering F 1 hybrid of sorghum. Euphytica 187, 411–420. https://doi.org/10.1007/s10681-012-0727-8.
Tanger, P., Klassen, S., Mojica, J.P., Lovell, J.T., Moyers, B.T., Baraoidan, M., Naredo, M.E.B., McNally, K.L., Poland, J., Bush, D.R., Leung, H., Leach, J.E., McKay, J.K., 2017. Field-based high throughput phenotyping rapidly identifies genomic regions controlling yield components in rice. Sci. Rep. 7, 1–8. https://doi.org/10.1038/srep42839.
Thapa, S., Zhu, F., Walia, H., Yu, H., Ge, Y., 2018. A novel LiDAR-Based instrument for high-throughput, 3D measurement of morphological traits in maize and sorghum. Sensors (Switzerland) 18. https://doi.org/10.3390/s18041187.
Topp, C.N., Iyer-pascuzzi, A.S., Anderson, J.T., Lee, C., Zurek, P.R., 2013. 3D phenotyping and quantitative trait locus mapping identify core regions of the rice genome controlling root architecture. Proc. Natl. Acad. Sci. 110, E1695–E1704. https://doi.org/10.1073/pnas.1304354110.
Tracy, S.R., Black, C.R., Roberts, J.A., Sturrock, C., Mairhofer, S., Craigon, J., Mooney, S.J., 2012. Quantifying the impact of soil compaction on root system architecture in tomato (Solanum lycopersicum) by X-ray micro-computed tomography. Ann. Bot. 110, 511–519. https://doi.org/10.1093/aob/mcs031.
Truong, S.K., McCormick, R.F., Rooney, W.L., Mullet, J.E., 2015. Harnessing genetic variation in leaf angle to increase productivity of sorghum bicolor. Genetics 201, 1229–1238. https://doi.org/10.1534/genetics.115.178608.
Upadhyaya, H.D., Wang, Y.-H., Sharma, S., Singh, S., 2012. Association mapping of height and maturity across five environments using the sorghum mini core collection. Genome 55, 471–479. https://doi.org/10.1139/g2012-034.
Virlet, N., Sabermanesh, K., Sadeghi-Tehran, P., Hawkesford, M.J., 2017. Field Scanalyzer: an automated robotic field phenotyping platform for detailed crop monitoring. Funct. Plant Biol. 44, 143–153. https://doi.org/10.1071/FP16163.
Wahabzada, M., Paulus, S., Kersting, K., Mahlein, A.K., 2015. Automated interpretation of 3D laserscanned point clouds for plant organ segmentation. BMC Bioinformatics 16, 1–11. https://doi.org/10.1186/s12859-015-0665-2.
Wang, H., Chen, G., Zhang, H., Liu, B., Yang, Y., Qin, L., Chen, E., Guan, Y., 2014. Identification of QTLs for salt tolerance at germination and seedling stage of Sorghum bicolor L. Moench. Euphytica 196, 117–127. https://doi.org/10.1007/s10681-013-1019-7.
Wang, H.L., Zhang, H.W., Du, R.H., Chen, G.L., Liu, B., Yang, Y.B., Qin, L., Cheng, E.Y., Liu, Q., Guan, Y.A., 2016. Identification and validation of QTLs controlling multiple traits in sorghum. Crop Pasture Sci. 67, 193–203. https://doi.org/10.1071/CP15239.
Wang, X., Singh, D., Marla, S., Morris, G., Poland, J., 2018. Field-based high-throughput phenotyping of plant height in sorghum using different sensing technologies. Plant Methods 14, 1–16. https://doi.org/10.1186/s13007-018-0324-5.
Watanabe, K., Guo, W., Arai, K., Takanashi, H., Kajiya-Kanegae, H., Kobayashi, M., Yano, K., Tokunaga, T., Fujiwara, T., Tsutsumi, N., Iwata, H., 2017. High-throughput phenotyping of sorghum plant height using an unmanned aerial vehicle and its application to genomic prediction modeling. Front. Plant Sci. 8, 1–11. https://doi.org/10.3389/fpls.2017.00421.
Yang, W., Guo, Z., Huang, C., Duan, L., Chen, G., Jiang, N., Fang, W., Feng, H., Xie, W., Lian, X., Wang, G., Luo, Q., Zhang, Q., Liu, Q., Xiong, L., 2014. Combining high-throughput phenotyping and genome-wide association studies to reveal natural genetic variation in rice. Nat. Commun. 5, 1–9. https://doi.org/10.1038/ncomms6087.
Zhang, D., Kong, W., Robertson, J., Goff, V.H., Epps, E., Kerr, A., Mills, G., Cromwell, J., Lugin, Y., Phillips, C., Paterson, A.H., 2015. Genetic analysis of inflorescence and plant height components in sorghum (Panicoidae) and comparative genetics with rice (Oryzoidae). BMC Plant Biol. 15, 1–15. https://doi.org/10.1186/s12870-015-0477-6.
Zhang, X., Huang, C., Wu, D., Qiao, F., Li, W., Duan, L., Wang, K., Xiao, Y., Chen, G., Liu, Q., Xiong, L., Yang, W., Yan, J., 2017. High-throughput phenotyping and QTL mapping reveals the genetic architecture of maize plant growth. Plant Physiol. 173, 1554–1564. https://doi.org/10.1104/pp.16.01516.
Zhang, Z., Ersoz, E., Lai, C.Q., Todhunter, R.J., Tiwari, H.K., Gore, M.A., Bradbury, P.J., Yu, J., Arnett, D.K., Ordovas, J.M., Buckler, E.S., 2010. Mixed linear model approach adapted for genome-wide association studies. Nat. Genet. 42, 355–360. https://doi.org/10.1038/ng.546.
Zhao, J., Mantilla Perez, M.B., Hu, J., Salas Fernandez, M.G., 2016. Genome-wide association study for nine plant architecture traits in sorghum. Plant Genome 9, 1–14. https://doi.org/10.3835/plantgenome2015.06.0044.
Zou, G., Zhai, G., Feng, Q., Yan, S., Wang, A., Zhao, Q., Shao, J., Zhang, Z., Zou, J., Han, B., Tao, Y., 2012. Identification of QTLs for eight agronomically important traits using an ultra-high-density map based on SNPs generated from high-throughput sequencing in sorghum under contrasting photoperiods. J. Exp. Bot. 63, 5451–5462. https://doi.org/10.1093/jxb/ers205.
Zurek, P.R., Topp, C.N., Benfey, P.N., 2015. Quantitative trait locus mapping reveals regions of the maize genome controlling root system architecture. Plant Physiol. 167, 1487–1496. https://doi.org/10.1104/pp.114.251751.